Available online at www.sciencedirect.com

SciVerse ScienceDirect

Ceramics International 39 (2013) 2481–2487

CERAMICS INTERNATIONAL

www.elsevier.com/locate/ceramint

Transparent polycrystalline $MgAl_2O_4$ ceramic fabricated by spark plasma sintering: Microwave dielectric and optical properties

Ping Fu[a,b,c], Wenzhong Lu[a,b,*], Wen Lei[a,b], Yong Xu[c], Xuehua Wang[c], Jiamin Wu[a,b]

[a]Department of Electronic Science and Technology, Huazhong University of Science and Technology, Wuhan 430074, China
[b]Key Laboratory of Functional Materials for Electronic Information(B) MOE, Huazhong University of Science and Technology, Wuhan 430074, China
[c]Department of Materials Science and Engineering, Wuhan Institute of Technology, Wuhan 430073, China

Received 30 June 2012; received in revised form 2 September 2012; accepted 2 September 2012
Available online 10 September 2012

Abstract

The optical properties and microwave dielectric properties of transparent polycrystalline $MgAl_2O_4$ ceramics sintered by spark plasma sintering (SPS) through homemade nanosized $MgAl_2O_4$ powders at temperatures between 1250 °C and 1375 °C are discussed. The results indicate that, with increasing sintering temperatures, grain growth and densification occurred up to 1275 °C, and above 1350 °C, rapid grain and pore growth occurred. The in-line light transmission increases with the densification and decreases with the grain/pore growth, which can be as high as 70% at the wavelength of 550 nm and 82% at the wavelength of 2000 nm, respectively. As the sintering temperature increases, $Q \times f$ and dielectric constant ε_r values increase to maximum and then decrease respectively, while τ_f value is almost independent of the sintering temperatures and remains between −77 and −71 ppm/°C. The optimal microwave dielectric properties ($\varepsilon_r = 8.38$, $Q \times f = 54{,}000$ GHz and $\tau_f = -74$ ppm/°C) are achieved for transparent $MgAl_2O_4$ ceramics produced by spark plasma sintering at 1325 °C for 20 min.

Keywords: Transparent $MgAl_2O_4$ ceramics; Spark plasma sintering; In-line transmittance; Microwave dielectric properties

1. Introduction

Magnesium aluminate spinel ceramics have isotropic crystal structure and have no birefringence, which exhibit excellent transparency in the visible- and IR-wavelength ranges while a full density or an extremely low porosity is attained [1,2]. At the same time, transparent $MgAl_2O_4$ ceramics are of great current interests on account of their versatile physical properties: high temperature resistance (melting point 2135 °C), strong corrosion resistance, excellent mechanical properties, thermal properties, and optoelectronic properties, both at normal and at elevated temperatures [3,4]. Transparent $MgAl_2O_4$ ceramics have been under development for many years, the primary focus has been especially on transparent armor, high temperature windows, infrared windows and advanced electromagnetic (EM) windows, etc [5,6]. However, the application of transparent $MgAl_2O_4$ ceramics is only focused on their optical performances; the microwave dielectric properties of transparent ceramics have been reported seldom. It is worth mentioning that $MgAl_2O_4$ spinel is a kind of fascinating microwave dielectric ceramic ($\varepsilon_r = 8.8$, $Q \times f = 68900$ GHz, and $\tau_f = -75$ ppm/°C) [7]. In many instances, both optical and microwave dielectric performances of transparent ceramics are required simultaneously such as the full-wave band transparent window materials with high transmittance in visible- and IR-wavelength even extending to microwave ranges. The transparent $MgAl_2O_4$ ceramics are one of the potential candidates for such applications. But the microwave dielectric properties of transparent $MgAl_2O_4$ ceramics have not been reported so far.

However, spinel is one of the hard-to-sinter ceramics, and hence transparent $MgAl_2O_4$ ceramics are difficult to be produced directly from a high-purity powder using conventional techniques such as pressureless sintering process. Spark plasma sintering (SPS) has been used to fabricate transparent

*Corresponding author at: Department of Electronic Science and Technology, Huazhong University of Science and Technology, Wuhan 430074, China.
E-mail address: lwz@mail.hust.edu.cn (W. Lu).

0272-8842/$ - see front matter © 2012 Elsevier Ltd and Techna Group S.r.l. All rights reserved.
http://dx.doi.org/10.1016/j.ceramint.2012.09.006

ceramics because it would enable one to achieve almost full densification within a few minutes by limiting grain growth and more uniform grain-size distribution than hot isostatic pressing (HIP) and hot pressing (HP) techniques. Several studies on SPS process have been conducted for improving the transparency of $MgAl_2O_4$ ceramics through optimizing the sintering conditions such as heating rate [8,9], sintering temperature [9], sintering aids [10], powder treatment [11] and pressure [12]. In particular, Bonnefont et al. [13] employed a low heating rate ≤ 10 °C/min and a sintering temperature 1300 °C, transparent polycrystalline $MgAl_2O_4$ ceramics with an in-line transmittance of 74% at wavelength of 550 nm and that of 84% at 2000 nm were fabricated by SPS, and a small average grain size of about 250 nm was obtained. The result is the best transmittance for transparent $MgAl_2O_4$ ceramics with the smallest grain size so far. But the process had an extortionate requirement for equipments because of its long time working, and it was difficult to be adopted in engineering applications.

In the present work, nanocrystalline $MgAl_2O_4$ powders were synthesized through a high-temperature calcination method firstly, and then fine grained transparent $MgAl_2O_4$ ceramics were prepared by a novel SPS process. The effects of SPS process parameters on the microstructures, optical properties and $Q \times f$ values of transparent $MgAl_2O_4$ ceramics were discussed in detail.

2. Experimental procedure

2.1. Material and preparation

The nanosized $MgAl_2O_4$ powders were prepared through a high-temperature calcination method [14]. High purity primary salts ($MgSO_4 \cdot 7H_2O$ and $NH_4Al \cdot (SO_4)_2 \cdot 12H_2O$ with a molar ratio of 1:2) were dissolved into an appropriate amount of de-ionized water and stirred fully. The mixed solution held in a quartz vessel was then put into a muffle oven for calcination at 1100 °C for 3 h. And then $MgAl_2O_4$ nanopowders can be obtained via screening. For SPS sintering (SPS-3.20MK II, Sumitomo Coal Mining Co., Ltd., Tokyo, Japan), the $MgAl_2O_4$ powders were filled into a graphite die with a 15-mm inner diameter. An optical pyrometer was used to measure the temperature of the graphite die surface. The sintering temperature and pressure were controlled via a programmable interface. The duty cycle of current pulse was set at 12/2. Under vacuum conditions (10 Pa), the temperature was first increased to 600 °C within 2 min and then further increased to 1100 °C in 5 min; then increased to the final sintering temperature of 1250–1375 °C with the heating rate of 10 °C/min. The dwell time for all experiments was 20 min. The pressure was applied by two steps: a uniaxial pressure of 28 MPa was pre-loaded and kept constant until a temperature of 1100 °C was reached and then increased to 80 MPa in 1 min and kept constant until the sintering end. After the sintering, the applied pressure was reduced to less than 28 MPa and the specimens were subsequently annealed at 1150 °C for 10 min to release the residual stress. Finally, a sintered column with a diameter of 15 mm and a thickness of 9 mm was obtained.

For properties characterization, the as-sintered samples were made into two parts: one is circular disk with size of $\Phi 15 \times 1.5\ mm^2$ for the in-line transmittance measurement and the other is column with size of $\Phi 15 \times 7\ mm^2$ for microwave dielectric properties measurement.

2.2. Microstructure characterization

The relative density of the SPSed columns was evaluated by using the Archimedes method. The phase identification of both $MgAl_2O_4$ powders and SPS sintered samples was carried out by X-ray diffractometer (XRD-7000, Shimadzu Corporation, Kyoto, Japan) working with Cu Ka radiation at 40 kV and 30 mA. SEM and TEM observation of $MgAl_2O_4$ powders was carried out with scanning electron microscopy (JSM-5510LV, JOEL Ltd. Tokyo, Japan) and transmission electron microscopy (JEM-2100F, JOEL Ltd. Tokyo, Japan), respectively. The fractured microstructure and grain shape of sintered $MgAl_2O_4$ ceramic were observed by scanning electron microscopy on the cross section of sample after thermal etching (at 1200 °C for 1 h in air). The grain size was calculated by measuring the average cross-section area per grain taken as spherical shape. According to literature [15], the measured grain size is an apparent one, so that it was multiplied by 1.225 to determine the true grain size.

2.3. Properties characterization

For optical properties measurement, both surfaces of the circular disks with thickness of 1.0 mm were mirror-polished with diamond polishing paste. The in-line transmittance T_{in} of sample was measured using a double-beam spectrophotometer (Lambda 35, PerkinElmer, Inc., California, USA) in the UV and visible light wavelength ranges ($\lambda = 190$–800 nm) and FT-IR/Raman spectrometer (VERTEX 70, Bruker Corp., Ettlingen, Germany) in the infrared wavelength ranges ($\lambda = 1150$–8000 nm).

For microwave dielectric properties measurement, the SPS sintered columns were heated at 900 °C for 1 h in air to decarburize. The dielectric constant (ε_r) and the unloaded $Q \times f$ value were measured in the TE_{011} mode by the Hakki and Coleman method [15] using an Agilent E8362B (Agilent Technologies, Inc., Santa Clara, USA) network analyzer and two parallel silver plates. The temperature coefficient of resonant frequency (τ_f) in the temperature range of 20–80 °C was calculated by formula (1)

$$\tau_f = \frac{f_2 - f_1}{f_1(T_2 - T_1)} \quad (1)$$

where f_1 and f_2 represent the resonant frequency at T_1 and T_2, respectively.

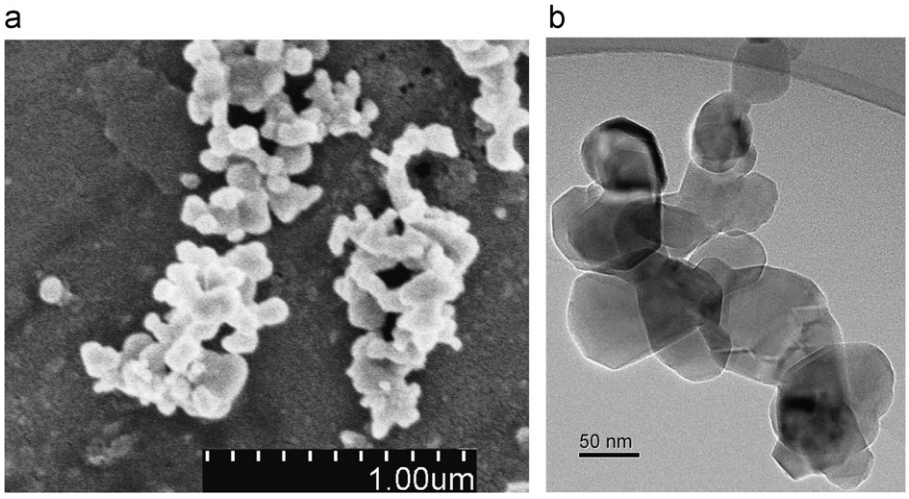

Fig. 1. SEM and TEM morphology of MAS powders synthesized at 1100 °C for 3 h: (a) SEM image and (b)TEM image.

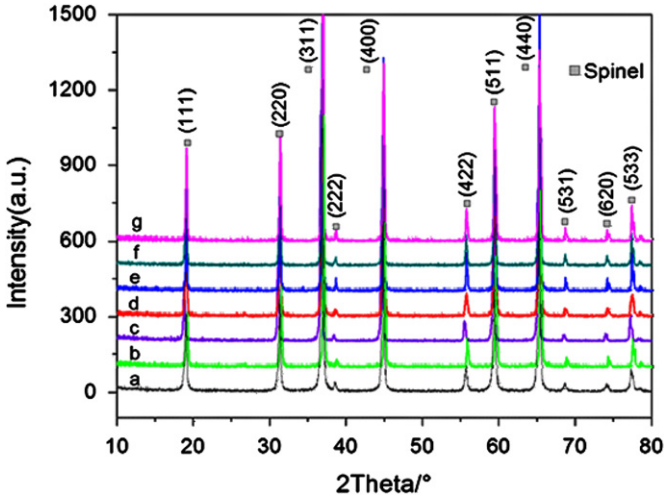

Fig. 2. XRD patterns of the $MgAl_2O_4$ powders and samples sintered at different temperatures for 20 min: (a) $MgAl_2O_4$ powders, (b) 1250 °C, (c) 1275 °C, (d) 1300 °C, (e) 1325 °C, (f) 1350 °C and (g) 1375 °C.

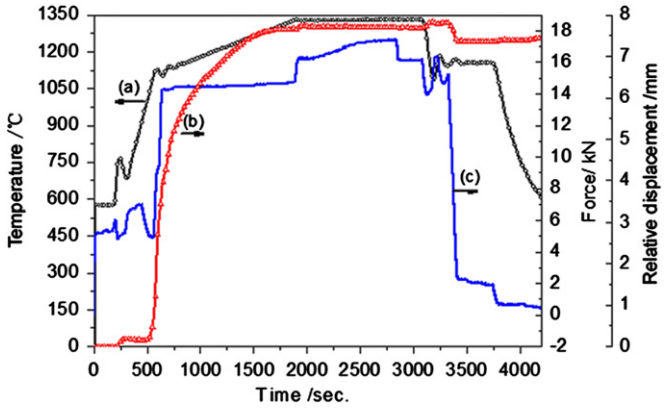

Fig. 3. Temperature and pressure regimes followed in the course of the SPS treatment. Also shown are the punch displacement curves, which reflects the length variation of the samples during the course of SPS process. (a) Sintering temperature, (b) relative displacement and (c) force.

3. Results and discussion

SEM and TEM image of $MgAl_2O_4$ powders through the high-temperature calcination method was shown in Fig. 1. As can be seen from Fig. 1, $MgAl_2O_4$ powders have spherical shape. A mean particle size calculated by averaging approximately 30 particles measurement is about 85 nm. It is clearly seen from SEM and TEM image that $MgAl_2O_4$ powders exhibit good dispersion, narrow size distribution and little agglomeration, which are necessary to obtain transparent ceramics.

Fig. 2 shows the XRD patterns of $MgAl_2O_4$ powder (Fig. 2(a)) and bulks sintered at different temperatures for 20 min (Fig. 2(b)–(g)). All diffraction peaks of $MgAl_2O_4$ powder were indexed as $MgAl_2O_4$ spinel (JCPDS card no. 21-1152). Compared to the diffraction peaks of powder, there is no phase change and no secondary phase occurred in the sintered samples. However, $MgAl_2O_4$ powder has slightly broadened diffraction peaks compared with those of bulks, i.e., the (311) peak has a full-width at half-maximum of 0.333 before sintering and 0.208 (1250 °C), 0.215 (1275 °C), 0.282 (1300 °C), 0.236 (1325 °C) and 0.165 (1375 °C) after sintering, which indicates the grain growth and high crystallinity of the SPSed samples.

The typical SPS process parameters sintered at 1325 °C, including the displacement of the upper punch, which reflects the shrinkage, i.e., densification of the sample, were shown in Fig. 3. Identical parameter profiles were applied to other samples sintered at different temperatures.

Fig. 3 shows the profiles of the parameters (temperature Fig. 3(a) and pressure Fig. 3(c)) that were applied in the course of SPS cycle. Fig. 3(b) describes the location of the punch, which is corresponding to the thermal expansion or shrinkage and the dimensional changes induced by sintering. From Fig. 3(b), it can be found that the punch displacement increases with the sintering temperature and

densification of power is gradually conducted. The punch displacement reaches the maximum and densification is completed when reaching the sintering temperature. Further increase of the temperature did not cause any additional densification. The other samples had the similar process curves.

Fig. 4 shows the polished discs sintered by SPS at different temperatures from 1250 to 1375 °C with a heating rate of 10 °C/min. At the temperature of 1250 °C, the border of the sample is opaque while the center is transparent. In the case of samples (b)–(e) the temperature was raised from 1275 to 1350 °C, the polished samples exhibit better transparency, and the text placed under the sample is clearly visible through the disc. With the further increasing of sintering temperature, the transparency of the sample decreases. At 1375 °C, the disc becomes translucent. All samples show the different degrees of blackish color due to carbon contamination and oxygen vacancies [11,16].

Fig. 5 shows the sintering temperature-dependent fracture microstructures of the SPSed samples. The SEM images show clearly that the SPS condition strongly affects the grain size and the residual porosity. Fig. 5(a) reveals that the grain sizes and morphologies were quite different between the center area and the border area (shown in the insert image) of the sample sintered at 1250 °C. In the center area, the densification degree is very high; it is accompanied by noticeable grain growth. On the other hand, in the border area there are still rounded grains showing just a minor increase in grain size. The reason which makes a remarkable difference is maybe the lower sintering temperature and the limited sintering time for $MgAl_2O_4$ ceramics. The sample sintered at 1275 °C has a dense microstructure and an average grain size of about 240 nm, which is slightly lower than 250 nm reported by Bonnefont et al. [13]. The fine grain size might be because of the starting nanopowders which allow a low sintering temperature to limit the grain growth. No residual pores can be identified in the thermally etched fractured surface (the insert image is the polished surface morphology of the sample after thermal etching) at 1275 °C. The average grain sizes increase from 240 nm to 2.5 μm as the temperature increases from 1275 °C to 1375 °C and the abnormal growth of crystal becomes significant at 1375 °C and the abrupt appearance of exaggerated grains can be found. Numerous residual pores and intergranular gap can be observed frequently at multiple grain junctions, as shown in Fig. 5(f), and the number of pores tends to increase with the sintering temperature. During sintering, most densification occurs by grain boundary sliding or

Fig. 4. Optical transparency of $MgAl_2O_4$ sintered at different temperatures for 20 min: (a) 1250 °C, (b) 1275 °C, (c) 1300 °C, (d) 1325 °C, (e) 1350 °C and (f) 1375 °C.

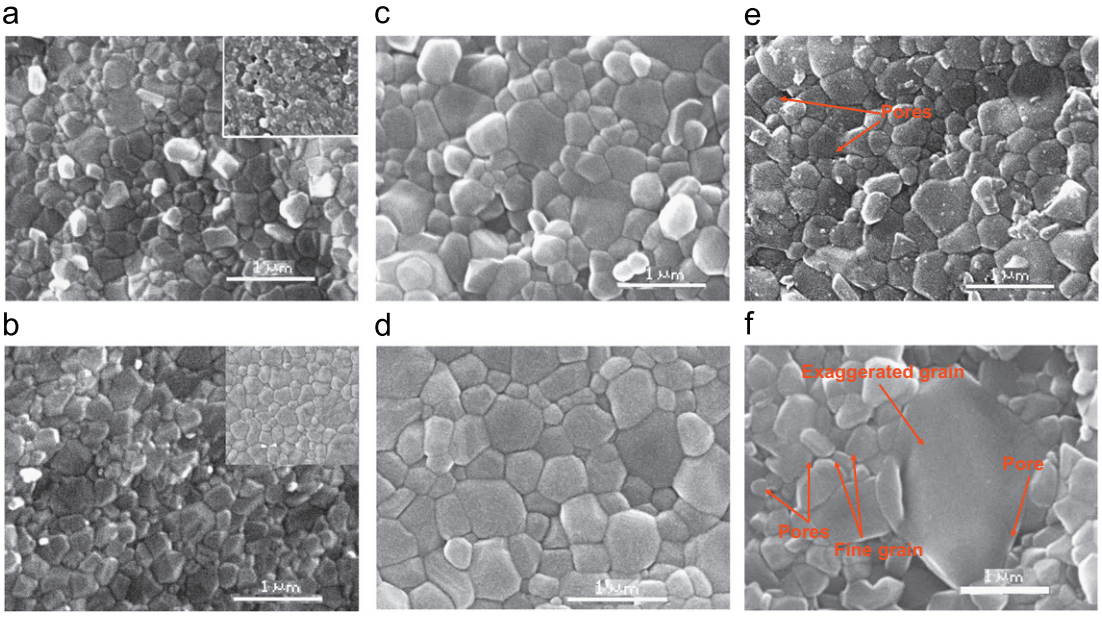

Fig. 5. SEM images of samples SPSed at different sintering temperatures and then thermally etched at 1200 °C for 1 h in air: (a) 1250 °C (the insert is the border of the sample), (b) 1275 °C, (c) 1300 °C, (d) 1325 °C, (e) 1350 °C and (f) 1375 °C.

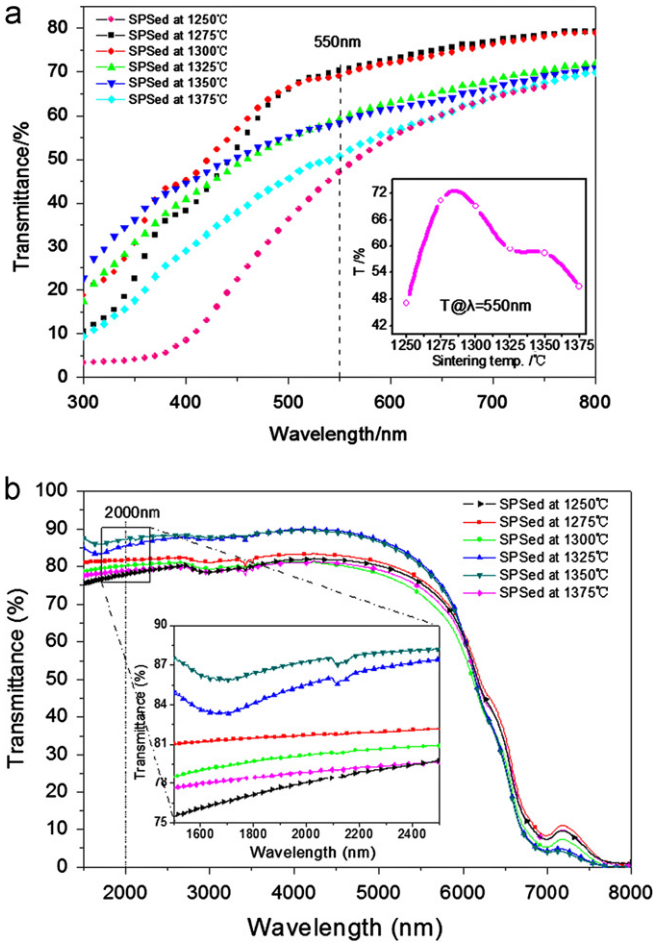

Fig. 6. In-line transmission T_{in} of polycrystalline $MgAl_2O_4$ sintered at different temperatures plotted as a function of wavelength λ. The sample thickness is 1.0 mm.

deformation. The pressure applied during SPS process increases the sliding or deformation rate, and grain boundary sliding at high temperatures cause accelerated grain growth. Pores might be formed due to the competition between grain growth and densification. The pores are likely due to the abnormal growth of crystal, which indicates that higher sintering temperatures (>1375 °C) can result in a translucent spinel (see Fig. 4) with large grain sizes and many residual pores. The results agree with the report by Morita et al. [9].

The in-line transmittance of SPSed samples is shown in Fig. 6. The in-line transmission evaluated at wavelengths of 550 nm ($T_{in,550}$) and 2000 nm ($T_{in,2000}$) were selected as representative of the samples in visible light and IR ranges. The insert in Fig. 6(a) shows the changes of $T_{in,550}$ with the increased sintering temperature. In the visible-wavelength range, $T_{in,550}$ is highly sensitive to the sintering temperature. For a heating rate of 10 °C/min, the samples exhibit a $T_{in,550}$ of 70% at $\lambda=550$ nm only for a soak time of 20 min at the low temperature of 1275 °C and 1300 °C. The $T_{in,550}$ determined in the present work has been compared with other experiment data reported in the literature by using Eq. (2) [13]:

$$RIT(d_2)=(1-R_s)\left(\frac{RIT(d_1)}{1-R_s}\right)^{\frac{d_2}{d_1}} \quad (2)$$

where R_s is the total normal surface reflectance (≈ 0.14) and RIT (d_1) is the in-line transmittance for a sample thickness $d1$, RIT (d_2) is the in-line transmittance for a sample thickness 1.0 mm. The result comparison was listed in Table 1.

The ideal result might be related to the fine grain size and fully dense microstructure [17]. At 1250–1375 °C, the $T_{in,550}$ initially increases and then decreases with the temperature. The deteriorated transmission can be attributed to the grain and pore growth. The over-sized grain boundary and the pores are the major factors causing serious light scattering [18]. In the present work, higher sintering temperatures (>1350 °C) lead to abnormal grains growth and residual pores, which made samples translucent, as demonstrated in Figs. 4 and 5.

Significant light scattering by pores is only available up to some specific wavelength range, so that, in the IR wavelength range, $T_{in,2000}$ is insensitive to the sintering temperature, the values are all above 79%. The $T_{in,2000}$ sintered at 1350 °C can reach a peak value of about 86%, which is very close to 87% achieved in $MgAl_2O_4$ single crystals. Using the home-made nanosized $MgAl_2O_4$ powders, the improved T_{in} obtained in the present work suggested that the mentioned novel process is beneficial for optical properties improvement of transparent $MgAl_2O_4$ ceramics sintered by SPS.

The relative density with standard deviation ($<0.5\%$) and dielectric constant of transparent $MgAl_2O_4$ ceramics as a function of sintering temperature are shown in Fig. 7. With increasing sintering temperature, the relative densities showed an initial increase, followed by a decrease. The maximum at 1275 °C was 99.89%. The reduction of the relative densities of the specimens was due to the appearance of pores resulting from an abnormal grain growth. In addition, the variation of ε_r was consistent with that of relative density. A maximum ε_r value of 8.42 was obtained for the specimen sintered at 1275 °C. The ε_r value in this work is lower than 8.8 measured by Surendran et al. [7].

Fig. 8 shows the variation of microwave dielectric properties of transparent $MgAl_2O_4$ ceramics as a function of sintering temperatures. With the increase of the sintering temperature, the $Q\times f$ values is increased at first and then is reduced after reaching the maximum value at

Table 1
Comparison of in-line transmission at wavelength of 550 nm of spinel ceramics sintered by SPS.

d_1 (mm)	RIT, $d1$ (%)	RIT, $d2$ (%)	References
1.8	47	61	[8]
1.79	51	64	[12]
3	74	82	[13]
1	70	70	Present work

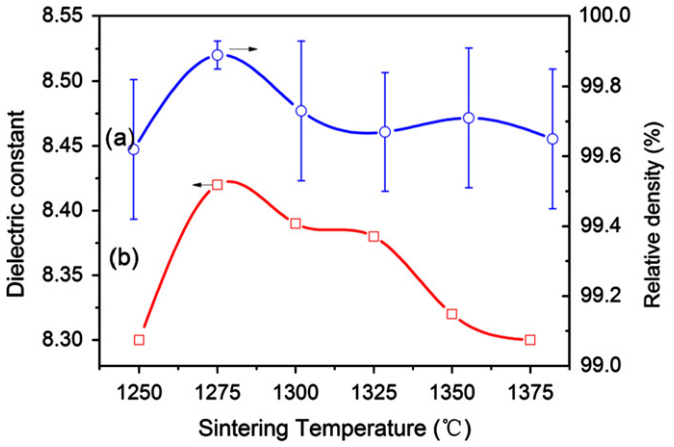

Fig. 7. Relative density and dielectric constant of transparent $MgAl_2O_4$ ceramics as a function of sintering temperatures: (a) ε_r and (b) relative density.

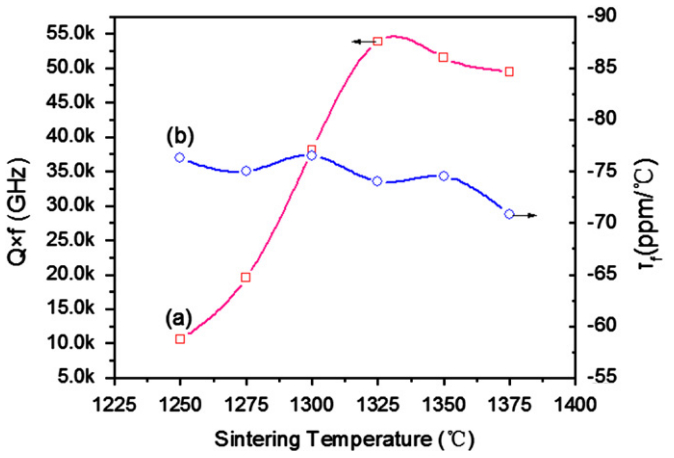

Fig. 8. $Q\times f$ and τ_f values of transparent $MgAl_2O_4$ ceramics SPSed at different temperatures: (a) $Q\times f$ and (b) τ_f.

1325 °C. The microwave dielectric losses in bulk ceramics fall into two categories: intrinsic and extrinsic [19–22]. The intrinsic loss is caused by anharmonic phonon decay processes in the pure crystal lattice while the extrinsic losses were mainly caused by ceramic density, crystallinity, inner stress and structural imperfections such as the pores, second phases, grain boundaries, etc [23]. The increase in sintering temperature is beneficial to the densification and crystallizability until the $Q\times f$ values reach the maximum. The further increase in sintering temperature will cause the appearance of abnormal grains and pores, and consequently lead to the reduction of the $Q\times f$ values. However, the reason that the peak value $Q\times f$ of transparent $MgAl_2O_4$ ceramic is lower than the reported values (as 68,900 GHz) of $MgAl_2O_4$ ceramic prepared via the traditional oxide route is due to oxygen vacancies and the carbon contamination caused by SPS processes. Fig. 8(b) illustrates the τ_f is almost independent of the sintering temperature and remains between −78.5 and −70.5 ppm/°C because of no compositional change. The average value of τ_f of transparent $MgAl_2O_4$ ceramics is similar to that of reported by Surendran et al. [7]. In this work, the best microwave dielectric properties of transparent $MgAl_2O_4$ ceramics is that $\varepsilon_r=8.38$, $Q\times f=54000$ GHz and $\tau_f=-74$ ppm/°C, which were achieved by the improved spark plasma sintering process at a temperature of 1325 °C and a soak time of 20 min.

4. Conclusion

Transparent $MgAl_2O_4$ ceramics have been fabricated through nanosized $MgAl_2O_4$ powders by using spark plasma sintering (SPS) technique at a temperature range from 1250 °C to 1375 °C. Light transmittance and microwave dielectric properties of the sintered $MgAl_2O_4$ ceramics were discussed in terms of its microstructure. The results showed that densification occurred up to a sintering temperature of 1275 °C, and above 1350 °C, rapid grain growth and pore growth occurred. The densification increased the light transmission, whereas the grain/pore growth reduced the in-line transmission. At the same time, the appearance of abnormal grains and pores deteriorated the $Q\times f$ values of transparent $MgAl_2O_4$ ceramics. The value of ε_r increased initially and then decreased with the increasing sintering temperature. And τ_f showed a linear dependence with the sintering temperature. The optimal microwave dielectric properties ($\varepsilon_r=8.38$, $Q\times f=54000$ GHz and $\tau_f=-74$ ppm/°C) can be obtained for transparent $MgAl_2O_4$ ceramics produced by spark plasma sintering at 1325 °C for 20 min.

Acknowledgment

This work was supported by the National Natural Science Foundation of China through Grant nos. 61172004 and 50902055. The provided supports are gratefully acknowledged.

References

[1] D.C. Harris, Window and dome technologies and materials IX window and dome technologies and materials IX, in: Proceedings of SPIE 5786 (2005) 1–22.
[2] T.J. Mroz, T.M. Hartnett, J.M. Wahl, L.M. Goldman, J. Kirsch, W.R. Lindberg, Recent advances in spinel optical ceramics, in: Proceedings of SPIE 5786 (2005) 64–70.
[3] D.C. Harris, Materials for Infrared Windows and Domes, Properties and Performance, SPIE Press, Bellingham, WA, 1999.
[4] S.M. Hosseini, Structural, electronic and optical properties of spinel $MgAl_2O_4$ oxide, Physica Status Solidi B 245 (2008) 2609–2615.
[5] A.C. Sutorik, G. Gilde, S. Kilczewski, P. Patel, J.M. Sands, Development of Transparent Ceramic Spinel ($MgAl_2O_4$) for Armor Applications, OSA/IODC/OF&T, 2010.
[6] G. Gilde, P. Patel, P. Patterson, Evaluation of hot pressing and hot isostastic pressing parameters on the optical properties of spinel, Journal of the American Ceramic Society 88 (2005) 2747–2751.
[7] K.P. Surendran, P.V. Bijumon, P. Mohanan, M.T. Sebastian, $(1-x)MgAl_2O_{4-x}TiO_2$ dielectrics for microwave and millimeter wave applications, Applied Physics A 81 (2005) 823–826.

[8] K. Morita, B.N. Kim, K. Hiraga, H. Yoshida, Fabrication of transparent $MgAl_2O_4$ spinel polycrystal by spark plasma sintering processing, Scripta Materialia 58 (2008) 1114–1117.
[9] K. Morita, B.N. Kim, K. Hiraga, H. Yoshida, Spark-plasma-sintering condition optimization for producing transparent $MgAl_2O_4$ spinel polycrystal, Journal of the American Ceramic Society 92 (2009) 1208–1216.
[10] N. Frage, S. Cohen, S. Meir, et al., Spark plasma sintering (SPS) of transparent magnesium–aluminate spinel, Journal of Materials Science 42 (2007) 3273–3275.
[11] B.N. Kim, K. Morita, J.H. Lim, K. Hiraga, H. Yoshida, Effects of preheating of powder before spark plasma sintering of transparent $MgAl_2O_4$ spinel, Journal of the American Ceramic Society 93 (2010) 2158–2160.
[12] C. Wang, Z. Zhao, Transparent $MgAl_2O_4$ ceramic produced by spark plasma sintering, Scripta Materialia 61 (2009) 193–196.
[13] G. Bonnefont, G. Fantozzi, S. Trombert, L. Bonneau, Fine-grained transparent $MgAl_2O_4$ spinel obtained by spark plasma sintering of commercially available nanopowders, Ceramics International 38 (2012) 131–140.
[14] T.C. Lu, X.H. Chang, J.Q. Qi, X.J. Luo, Low-temperature high-pressure preparation of transparent nanocrystalline $MgAl_2O_4$ ceramics, Applied Physics Letters 88 (2006) 213120–213123.
[15] B.W. Hakki, P.D. Coleman, A dielectric resonator method of measuring inductive capacities in the millimeter range, IEEE Transactions, Microwave Theory and Techniques 8 (1960) 402–410.
[16] G. Bernard-Granger, N. Benameur, C. Guizarda, M. Nygren, Influence of graphite contamination on the optical properties of transparent spinel obtained by spark plasma sintering, Scripta Materialia 60 (2009) 164–167.
[17] R. Apetz, M.P.B. Bruggen, Transparent alumina: a light-scattering model, Journal of the American Ceramic Society 86 (2003) 480–486.
[18] B.N. Kim, K. Hiraga, S. Grasso, et al., High-pressure spark plasma sintering of MgO-doped transparent alumina, Journal of the Ceramic Society of Japan 120 (2012) 116–118.
[19] J.W. Choi, C.Y. Kang, S.J. Yoon, H.J. Kim, H.J. Jung, Microwave dielectric properties of $Ca[(Li_{1/3}Nb_{2/3})_{1-x}M_x]O_{3-\delta}$ (M=Sn, Ti) ceramics, Journal of Materials Research 14 (1999) 3567–3570.
[20] A. Templeton, X. Wang, S.J. Penn, S.J. Webb, N.M. Cohen, L.F. Alford, Microwave dielectric loss of titanium oxide, Journal of the American Ceramic Society 83 (2000) 95–100.
[21] V.B. Braginsky, V.S. Ilchenko, K.S. Bagdassarov, Experimental-observation of fundamental microwave-absorption in high-quality dielectric crystals, Physics Letters A 120 (1987) 300–305.
[22] V.L. Gurevich, A.K. Tagantsev, Intrinsic dielectric loss in crystals, Advances in Physics 40 (1991) 719–767.
[23] A. Feteira, D.C. Sinclair, M.T. Lanagan, Structure and microwave dielectric properties of $Ca_{1-x}Y_xTi_{1-x}Al_xO_3$ (CYTA) ceramics, Journal of Materials Research 20 (2005) 2391–2399.